

Phonon line shape in disordered A_3C_{60} ($A = K, Rb$)

J.E. Han⁽¹⁾, O. Gunnarsson⁽¹⁾ and V. Eyert^(1,2)

⁽¹⁾ *Max-Planck-Institut für Festkörperforschung, D-70506 Stuttgart, Germany*

⁽²⁾ *Institut für Physik, Universität Augsburg, D-86135 Augsburg, Germany*

(February 1, 2008)

We present a calculation of the H_g phonon self-energy for a model of A_3C_{60} ($A = K, Rb$). The orientational disorder of the C_{60} molecules is included, and the lowest order self-energy diagram is considered. The calculations illustrate that due to the violation of momentum conservation by the orientational disorder, Raman scattering can measure the decay of a phonon in an electron-hole pair, allowing the estimate of the electron-phonon coupling from such experiments. Comparison with experimental line shapes further provides support for a local correlation of the molecular orientations, with neighboring molecules preferentially having orientations differing by a 90° rotation.

I. INTRODUCTION

It is essential for the understanding of the alkali-doped fullerenes A_3C_{60} ($A = K, Rb$) to obtain reliable estimates of the strength λ of the electron-phonon interaction. In metallic systems, such as A_3C_{60} , a phonon can decay in an electron-hole pair. This decay leads to an extra width of the phonon. It was pointed out by Allen¹ that λ can be estimated from the average of this extra width (γ_{ph}) over all \mathbf{q} -vectors. This width can be measured in, e.g., neutron scattering.² It is, however, not easy to extract accurate values of λ from such experiments for C_{60} . Raman scattering provides an interesting alternative, since it gives a high resolution and since the Raman active modes (A_g and H_g) are the modes which couple to the electrons in the partly filled t_{1u} band.

In the context of the fullerenes, it was early pointed out that for the ordered system energy and momentum conservation forbids the decay of a $\mathbf{q} = 0$ intramolecular phonon in an intraband electron-hole pair excitation.³ Due to the long wave length of the photons used in Raman scattering, this experiment would then not be appropriate for extracting λ , since $\mathbf{q} \approx 0$ phonons are excited. A_3C_{60} has, however, strong orientational disorder, with each molecules taking essentially randomly one out of two preferred directions.⁴ Schlüter *et al.* therefore emphasized that decay of a H_g phonon is nevertheless possible, since \mathbf{q} -conservation is violated,⁵ while the decay of a $\mathbf{q} = 0$ A_g phonon is not possible.⁶ It was later assumed that the violation of \mathbf{q} -conservation is so efficient, that Raman scattering actually measures an average of H_g phonons at all \mathbf{q} -vectors,⁷ as assumed in the Allen formula. Recently, however, the applicability of Allen's formula was anew put into question.⁸ It was concluded that for a \mathbf{q} -independent interaction, there is no broadening of the $\mathbf{q} = 0$ H_g mode, and that the broadening of this mode is entirely due to the \mathbf{q} -dependence of the coupling. This led to a drastic reinterpretation of the coupling constants derived from earlier Raman measurements.⁹ Explicit calculations have been performed for orientation-

ally disordered systems, but the broadening of the $\mathbf{q} = 0$ modes was not studied.¹⁰ Therefore, although Allen's formula is the basis for deductions of λ from Raman data, its validity for disordered A_3C_{60} has to our knowledge never been explicitly tested. The purpose of this paper is to perform such a test.

In Sec. II we present our model and the formalism, the results are presented and discussed in Sec. III and we give a summary in Sec. IV.

II. MODEL AND FORMALISM

We consider a model which includes the partly occupied t_{1u} band. There are three t_{1u} orbitals on each C_{60} molecule i , which are connected by hopping matrix elements t

$$H^{\text{el}} = \sum_{i\sigma} \sum_{m=1}^3 \varepsilon_{t_{1u}} n_{im\sigma} + \sum_{\langle ij \rangle \sigma mm'} t_{ijmm'} \psi_{im\sigma}^\dagger \psi_{jm'\sigma} \quad (1)$$

The orientational disorder⁴ has been built into the matrix elements $t_{ijmm'}$.¹¹⁻¹³ We want to describe the coupling to the intramolecular five-fold degenerate H_g Jahn-Teller modes. To describe the electron-phonon interaction, we use the Hamiltonian

$$H^{\text{el-ph}} = \omega_{ph} \sum_{i,\mu=1}^5 (b_{i\mu}^\dagger b_{i\mu} + \frac{1}{2}) + \frac{g}{2} \sum_{\mu=1}^5 \sum_{i\sigma} \sum_{m=1}^3 \sum_{m'=1}^3 V_{mm'}^{(\mu)} \psi_{im\sigma}^\dagger \psi_{im'\sigma} (b_{i\mu} + b_{i\mu}^\dagger), \quad (2)$$

where ω_{ph} is the a phonon frequency, $b_{i\mu}$ annihilates a phonon with quantum number μ on site i , g is an overall coupling strength and $V_{mm'}^{(\mu)}$ are dimensionless coupling

constants^{14,15} given by symmetry;

$$V^{(\mu)} = \begin{pmatrix} 1 & 0 & 0 \\ 0 & 1 & 0 \\ 0 & 0 & -2 \end{pmatrix}, \sqrt{3} \begin{pmatrix} 1 & 0 & 0 \\ 0 & -1 & 0 \\ 0 & 0 & 0 \end{pmatrix},$$

$$\sqrt{3} \begin{pmatrix} 0 & 1 & 0 \\ 1 & 0 & 0 \\ 0 & 0 & 0 \end{pmatrix}, \sqrt{3} \begin{pmatrix} 0 & 0 & 0 \\ 0 & 0 & 1 \\ 0 & 1 & 0 \end{pmatrix}, \sqrt{3} \begin{pmatrix} 0 & 0 & 1 \\ 0 & 0 & 0 \\ 1 & 0 & 0 \end{pmatrix}, \quad (3)$$

for $\mu = 1, \dots, 5$ respectively. The electron-phonon coupling constant λ is then given by^{14,15}

$$\lambda = \frac{5}{3} N(0) \frac{g^2}{\omega_{ph}}, \quad (4)$$

where $N(0)$ is the density of states (DOS) per spin at the Fermi energy. We have assumed that the H_g modes are local Einstein modes with a local coupling to the electrons. Since these modes are intramolecular and since the interaction between the C_{60} molecules is very weak, these assumptions should be very good. Actually, explicit calculations of the phonon dispersion curves for the H_g modes find that the dispersion is extremely small.¹⁶

To describe the broadening of the phonon, we calculate the phonon self-energy due to the electron-phonon interaction. We consider the lowest order self-energy, expressed in terms of the zeroth order electron and phonon Green's functions. This is the formalism used by Allen.¹ In the present case, the phonon energy is not much smaller than the bandwidth and the validity of Migdal's theorem is therefore questionable. Contributions beyond the lowest order self-energy diagram may therefore be important. The on-site Coulomb interaction is large in these systems, which are believed to be close to a Mott transition.¹⁷ For simplicity, we have here nevertheless neglected corrections to Migdal's theorem and effects of the Coulomb interaction.

We diagonalize the electronic part H^{el} of the Hamiltonian. The eigenstates are labelled by n , the eigenvalues are ε_n and the corresponding zeroth order electron Green's function is $G_n^0(\omega)$. The phonon self-energy is then

$$\Pi_{\alpha, \alpha'}(\omega) = -i \sum_{\sigma} \sum_{nm} \int \frac{d\omega'}{2\pi} g_{nm}^{\alpha} g_{nm}^{\alpha'} G_n^0(\omega') G_m^0(\omega + \omega'), \quad (5)$$

where $\alpha \equiv (i\mu)$ labels a combined site and phonon degeneracy index and g_{nm}^{α} is the matrix element of the coupling to the phonon α between the one-particle states n and m . The frequency integral can be performed analytically, giving

$$\Pi_{\alpha, \alpha'}(\omega) = 2 \sum_{nm} g_{nm}^{\alpha} g_{nm}^{\alpha'} \frac{f_m - f_n}{\varepsilon_m - \varepsilon_n - \omega + i\eta}, \quad (6)$$

where $f_n \equiv f(\varepsilon_n)$ is the Fermi function, η an infinitesimal positive number. In the present calculation, we used

$\eta = 0.0004$ eV, comparable to experimental resolution⁹ and much smaller than ω_{ph} and γ_{ph} .

The phonon Green's function D is given by

$$D^{-1} = [D^0]^{-1} - \Pi, \quad (7)$$

where a matrix notation is understood and the noninteracting phonon Green's function is given by

$$D_{\alpha\alpha'}^0(\omega) = \frac{2\omega_{ph}}{\omega^2 - \omega_{ph}^2 + i\eta} \delta_{\alpha\alpha'}. \quad (8)$$

We introduce the reduced Green's function in momentum space

$$\tilde{D}_{\mu, \mu'}(\mathbf{q}, \omega) = \frac{1}{N} \sum_{ij} \sum_{\nu} e^{i\mathbf{q} \cdot (\mathbf{R}_i - \mathbf{R}_j)} c_{\mu\nu}^{ij} D_{i\nu, j\mu'}(\omega), \quad (9)$$

where N is the number of molecules in the cluster, $c_{\mu, \nu}^{ij}$ the scattering coefficients with proper symmetry factors corresponding to the specific experiment, as discussed in the Appendix.

We compute the coefficients $c_{\mu, \nu}^{ij}$ for Raman scattering experiments. We consider electronic transitions within the t_{1u} and t_{1g} bands, assuming that the photon energy is larger than the t_{1u} - t_{1g} splitting. To obtain a simple result, we make the approximation that the hopping matrix elements are small. Calculations using realistic hoppings give qualitatively similar results. Details of the derivation are given in the Appendix. Then, we have an expression for $c_{\mu\nu}^{ij}$ which only depends on μ, ν and molecular orientations $o(i)$ at sites i, j , ($o(i) = \pm 1$).

Between molecules with the same orientation, *i.e.*, $o(i) = o(j)$,

$$c_{\mu, \mu}^{ij} = 1 \text{ (all } \mu), \quad (10)$$

For $o(i) = 1, o(j) = -1$,

$$c_{11}^{ij} = -c_{22}^{ij} = -c_{33}^{ij} = -c_{45}^{ij} = c_{54}^{ij} = 1, \quad (11)$$

and for $o(i) = -1, o(j) = 1$,

$$c_{11}^{ij} = -c_{22}^{ij} = -c_{33}^{ij} = c_{45}^{ij} = -c_{54}^{ij} = 1. \quad (12)$$

Finally,

$$c_{\mu\mu}^{ij} = 0, \text{ otherwise.} \quad (13)$$

In the following we are interested in $\tilde{D}_{\mu, \mu}(\mathbf{q} = 0, \omega)$, since in Raman scattering the coupling is to $\sum_{\mu} \tilde{D}_{\mu, \mu}(\mathbf{q} = 0, \omega)$, and in

$$D^{\text{local}}(\omega) = \frac{1}{N} \sum_{\mathbf{q}} \sum_{\mu} \tilde{D}_{\mu, \mu}(\mathbf{q}, \omega). \quad (14)$$

In the $\mathbf{q} = 0$ phonon Green's function momentum conservation is considered, to the extent that it survives the

orientational disorder. On the other hand, the usage of D^{local} instead implies an assumption that the orientational disorder has completely destroyed momentum conservation and that we therefore can average over all momenta as in neutron scattering. The spectral functions are defined as the imaginary part of the Green's functions, *i.e.*, $\rho_{\mu}(\mathbf{q}, \omega) = -(1/\pi)\text{Im}\bar{D}_{\mu,\mu}(\mathbf{q}, \omega)$.

Allen's formula for the phonon broadening γ_{ph} (full width at half maximum (FWHM)), can be derived from Eq. (6) in the limit of $w_{ph} \ll W$ and by ignoring the momentum conservation, and it is given by

$$\gamma_{ph} = \frac{2\pi}{3}g^2\omega_{ph}N(0)^2 = \frac{2\pi}{5}\lambda\omega_{ph}^2N(0). \quad (15)$$

The phonon level shift estimated from the real part of the self-energy can be expressed as

$$\Delta\omega_{ph} = \left(-2\ln 2 + \frac{7}{9}(w_{ph}N(0))^2\right)g^2N(0), \quad (16)$$

for a flat DOS. The second term in the bracket is the correction of order $(\omega_{ph}/W)^2$.

III. RESULTS

We have performed calculations for clusters with 256 atoms on an fcc lattice and with periodic boundary conditions. We take into account the fact that neighboring molecules tend to anti-align,¹⁸ due to the hopping integral being stronger for such configurations.^{11,13} We control the randomness of orientation by introducing an Ising-type nearest neighbor antiferromagnetic interaction for the two preferred orientations, *i.e.*, $E_{rot} = \mathcal{N}^{-1}\sum_{\langle i,j \rangle} o(i)o(j)$ with \mathcal{N} the number of nearest neighbor pairs. First we start from a truly random orientation and then *anneal* the system to any desired randomness by using a fictitious temperature. Since the fcc lattice is frustrated, there are many “antiferromagnetic” (AFM) states which minimize E_{rot} at $E_{rot,min} = -1/3$. Therefore even a perfectly annealed system retains a certain disorder, as can be seen in the electron density of states. Then the phonon spectral functions are averaged over many sets of orientational configurations.

The phonon spectral functions for the scattering vector $\mathbf{q}=0$ and the local (summed over all \mathbf{q}) spectral function are plotted in Fig. 1 for different orientational disorders. The phonon line widths for $\mathbf{q}=0$ (solid lines) and local (dashed lines) spectral functions are about the same over a large range of disorder (different values of E_{rot}). This shows that the orientational disorder effectively breaks momentum conservation, and it supports the assumption that the Raman scattering experiment can give an estimate of the electron-phonon coupling. On the other hand, a calculation for a periodic “ferro-magnetically” ordered system gave two unbroadened peaks due to energy and momentum conservation, as will be discussed later.

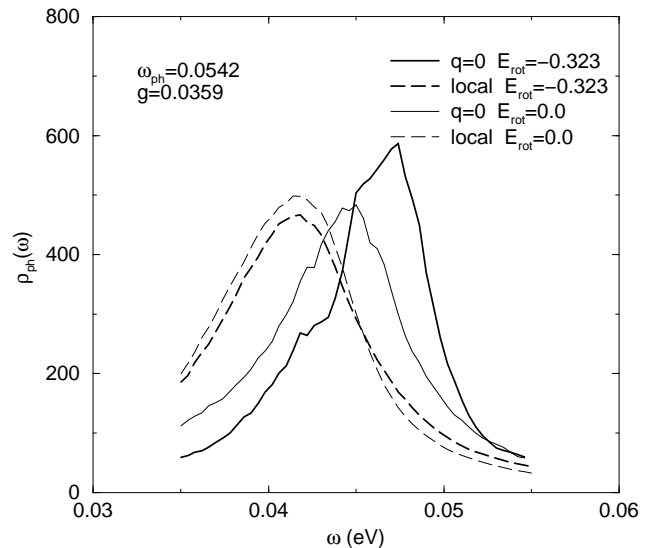


FIG. 1. $\mathbf{q}=0$ and local phonon spectral functions at different rotational energies. The local spectral functions (dashed lines) show structureless profile with the weak dependence on the rotational energy. The $\mathbf{q}=0$ spectral functions significantly depend on the disorder structure of the fcc C_{60} lattice.

The validity of Allen's formula, Eq. (15), is explicitly tested by changing the phonon frequency w_{ph} . Since the self-energy is trivially proportional to g^2 , we concentrated on the linear dependence of γ_{ph} on w_{ph} for a fixed g . The numerical estimates for the broadening γ_{ph} and the level shift $\Delta\omega$ are computed by fitting the $\mathbf{q}=0$ spectral functions to a single-pole phonon spectral function

$$\rho_{fit}(\omega) = -\text{Im} \frac{A/\pi}{\left(\frac{\omega^2 - \omega_{ph}^2}{2\omega_{ph}}\right)^2 - \Delta\omega + i\gamma_{ph}}, \quad (17)$$

where A is the total spectral weight.¹⁹ Although the numerical spectral functions are far from being single-pole structured, the peak position and the FWHM, γ_{ph} , can be understood in an average sense.

The widths and shifts obtained from these fits are compared with the results of Allen's formula in Table I. In Allen's formula we have used $N(0) = 6.2\text{eV}^{-1}$, which is the appropriate value for our model of A_3C_{60} . The coupling constant g was set to 0.03 eV. We find that Allen's formula is reasonably well reproduced from the $\mathbf{q}=0$ spectral functions. The discrepancies between the numerical and Allen's estimated values range within 20-40 %, which we attribute mainly to finite size effects. The phonon broadening decreased as the number of sites was increased. Also note that γ_{ph} shows a poorer agreement for small values of ω_{ph} , where finite size effects become more pronounced due to the small number of particle-hole pairs with excitation energy less than ω_{ph} . Due to computational limitations, we have considered a maximum number of 256 sites although the convergence with respect to the system size is not good enough for a systematic finite size scaling analysis.

We have calculated the Raman scattering spectra for systems close to the local minima of antiferromagnetically ordered orientations by using realistic parameters for the coupling constant g obtained from the photoemission spectra analysis²¹. We then discuss the relevance of our calculation to Raman scattering experiments.⁹ We have performed the calculations for the first two H_g -modes at frequencies of 0.0336 and 0.0542 eV (270, 432 cm⁻¹, respectively) and have taken average over 10 sets of rotational configurations for $E_{rot} = -0.323$, close to the AFM minima at $E_{rot} = -0.333$.

For the first two H_g modes the fitted γ_{ph} 's are 13, 47 cm⁻¹ for $\omega_{ph}=270, 432$ cm⁻¹, respectively. These values differ by almost a factor of 2 from the experimental estimates at 20 and 21 cm⁻¹, respectively.⁹ This illustrates the fact that photoemission and Raman scattering give rather different estimates of the distribution of the coupling strength for the low-lying phonons.¹⁷ The calculated Raman spectrum for $H_g(2)$ mode is shown in Fig. 2. The total spectrum can be resolved in two major peaks from the first two ($\mu = 1, 2$ at A) and the last three²² ($\mu = 3, 4, 5$ at B) modes of the phonon. This leads to a spectrum which agrees reasonably well with the low-energy part of the spectrum in Ref. 9, in the sense that the spectrum is strongly skewed towards higher energies and has additional structures. This provides support for the belief^{11,13,18} that there is a local 'antiferromagnetic' correlation, since the agreement with experiment is better than for the random orientation. The two narrow high frequency peaks in the experimental spectrum seem, however, to be beyond our treatment.

To discuss the phonon level splitting into a doublet ($\mu = 1, 2$) and a triplet ($\mu = 3, 4, 5$), we define the reduced phonon self-energy at $\mathbf{q}=0$ in analogy to the reduced phonon Green's function $\tilde{D}_{\mu,\mu'}(\mathbf{q}=0, \omega)$ as

$$\tilde{\Pi}_{\mu,\mu'}(\mathbf{q}=0, \omega) = \frac{1}{N} \sum_{ij} \sum_{\nu} c_{\mu\nu}^{ij} \Pi_{i\nu,j\mu'}(\omega), \quad (18)$$

which is the corresponding self-energy for $\tilde{D}_{\mu,\mu'}(\mathbf{q}=0, \omega)$. (See Appendix.) The real part of $\tilde{\Pi}_{\mu,\mu}(0, \omega_{ph})$ agrees very well with the phonon level shift previously obtained by fitting the spectral function for $\tilde{D}_{\mu,\mu}(0, \omega)$. The level shifts are better understood by investigating the imaginary part of $\tilde{\Pi}_{\mu,\mu}(0, \omega)$, which, related to the real part by the Kramers-Kronig relation, gives the excitation spectrum responsible for the perturbational level shift. Spectra of $\text{Im}\tilde{\Pi}_{\mu,\mu}(0, \omega)$ extend from 0 to the bandwidth and show different shapes for the doublet and triplet. For orientational configurations close to the AFM minima, those for the doublet are skewed to higher energy giving the smaller contribution to the level shift while those for triplets are skewed to lower energy leading to the larger level shift. For random orientations, the two spectra show essentially the same shape as the system size is increased.

The imaginary part of $\tilde{\Pi}_{\mu,\mu}(0, \omega)$ represents the spectral distribution of coupling of μ -th phonon to electron-

hole pair excitations. More specifically, $\tilde{\Pi}_{\mu,\mu}(0, \omega)$ can be written as the energy spectrum of the state for the uniformly distorted field, $|\phi^{(\mu)}\rangle$, due to μ -th Jahn-Teller phonon mode;

$$\text{Im}\tilde{\Pi}_{\mu,\mu}(0, \omega) = \frac{\pi g^2}{4} \sum_{\sigma, \alpha, \beta}' \left| \langle \alpha, \beta | \phi^{(\mu)} \rangle \right|^2 \delta(\omega - \varepsilon_{\alpha} + \varepsilon_{\beta}), \quad (19)$$

where the summation is over the electron-hole pair states $|\alpha, \beta\rangle$ ($\varepsilon_{\alpha} > \varepsilon_F$, $\varepsilon_{\beta} < \varepsilon_F$ with the Fermi energy ε_F) and

$$|\phi^{(\mu)}\rangle = \sum_{imm'\sigma} \tilde{\psi}_{im\sigma}^{\dagger} V_{mm'}^{(\mu)} \tilde{\psi}_{im'\sigma} |0\rangle, \quad (20)$$

with the non-interacting Fermi sea $|0\rangle$. $\tilde{\psi}_{im\sigma}$ is the annihilation operator for the orbital pointing along the m -th principal axis, *not* along the molecular orientation, *i.e.*, $\tilde{\psi}_{im\sigma} = \psi_{im\sigma}$ for $o(i) = 1$ and $\tilde{\psi}_{ix\sigma} = \psi_{iy\sigma}$, $\tilde{\psi}_{iy\sigma} = -\psi_{ix\sigma}$ and $\tilde{\psi}_{iz\sigma} = \psi_{iz\sigma}$ for $o(i) = -1$. The energy expectation value of the distorted field can be related to the first moment of $\text{Im}\tilde{\Pi}_{\mu,\mu}(0, \omega)$ as

$$\frac{\langle \phi^{(\mu)} | H^{el} | \phi^{(\mu)} \rangle}{\langle \phi^{(\mu)} | \phi^{(\mu)} \rangle} = E_0 + \frac{\int_0^{\infty} \omega \text{Im}\tilde{\Pi}_{\mu,\mu}(0, \omega) d\omega}{\int_0^{\infty} \text{Im}\tilde{\Pi}_{\mu,\mu}(0, \omega) d\omega}, \quad (21)$$

where E_0 is the ground state energy of non-interacting electrons. As expected near the AFM local minima, $\langle \phi^{(\mu)} | H^{el} | \phi^{(\mu)} \rangle / \langle \phi^{(\mu)} | \phi^{(\mu)} \rangle$ has smaller value for the doublet and larger value for the triplet.

The Jahn-Teller phonon couples to the distortion of the electronic density. For the doublet modes, the phonons couple to the density distortion along the principal axes, *e.g.*, for $\mu = 1$, $(b_{i1}^{\dagger} + b_{i1})$ couples to $(n_{ix} + n_{iy} - 2n_{iz})$, the distortion elongated or squeezed along z -axis. Similarly, the triplet phonons couple to distortions along diagonal directions in xy, yz, zx -planes *e.g.*, for $\mu = 3$, $(b_{i3}^{\dagger} + b_{i3})$ couples to $(n_{i\tilde{x}} - n_{i\tilde{y}})$ where \tilde{x}, \tilde{y} axes are rotated from x, y -axes by 45° along z -axis. Therefore, the distortion for $\mu = 3, 4, 5$ tend to distribute more electrons along the in-plane diagonal directions, which are the strongest bonding directions for t_{1u} -orbitals in the fcc lattice.¹² Furthermore, upon the inter-site coherence close to AFM minima, the distortions from neighbors add up constructively along the strongest bonding direction to give the energy gain for the triplet phonons, leading to the skewedness toward the low energy.

It has been suggested⁹ that the locally broken cubic symmetry, due to the orientational disorder, could lead to a splitting of all five levels in the H_g modes. However within our model, it seems unlikely that the local energy splittings survive after averaging over all sites. Rather, the calculation indicates that the local energy splittings contribute to the broadening of levels, not to collective $\mathbf{q}=0$ modes which survive disorder. We observe that the first two peaks in the experiment of Winter *et al.* could

reflect states in isolated C_{60} , since their observed energy shifts from the undoped C_{60} values are too small compared to estimates of the phonon self-energy from the lowest order diagram and sometimes even have different signs. Considering the narrowness of these peaks, they could result from a many-electron molecular states, due to effects neglected in this study, and with a very weak coupling to the surrounding.

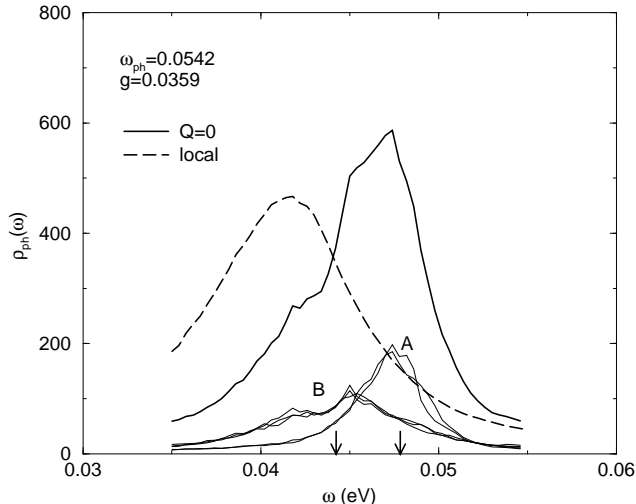


FIG. 2. Phonon spectral functions for realistic parameter $w_{ph} = 0.0542$ eV and $g = 0.0359$ eV for $H_g(2)$ mode. The thick solid line shows the $\mathbf{q}=0$ phonon spectral function as can be observed in Raman scattering. The spectrum has underlying structures which can be resolved to two peaks A and B by plotting projected spectral functions for each phonon modes (thin lines). The local phonon spectral function (dashed line) shows no such underlying structure. For comparison, the peak positions for a completely ordered periodic lattice are marked by arrows.

Our results are in strong contrast to the results of Aksenov and Kabanov.⁸ They studied the problem in a model where the orientational disorder was described by a relaxation rate, leading to an imaginary self-energy in the electron Green's function. However, the breaking of the translational symmetry was not explicitly included, and momentum conservation was assumed in evaluating various diagrams. The orbital degeneracy was also neglected. It was concluded that for a \mathbf{q} -independent electron-phonon coupling there is no broadening of a H_g phonon and that the broadening is entirely due to the dependence of the coupling on the angle of \mathbf{q} . This is in strong contrast to the results above, where we find that a \mathbf{q} -independent coupling gives a substantial broadening, provided that the violation of the translational symmetry is included explicitly. As was discussed in Sec. II, the \mathbf{q} -dependence of the coupling should be very weak, and the effect discussed in Ref. 8 not very important.

Aksenov and Kabanov⁸ were not able to obtain the angular dependence of the coupling constants and therefore they could not deduce the absolute magnitude of

the coupling constants from Raman experiments, but instead estimated the relative coupling constants from Raman experiments. To obtain absolute estimates, they used coupling constants deduced²⁰ from photoemission²¹ for a free C_{60} molecule and arbitrarily assumed that the coupling constant to the lowest mode is correct. Had they instead, equally arbitrarily, assumed that the coupling to the third mode is correct, all values of λ_ν would have been about a factor of two larger and if they had assumed that the deduced²⁰ coupling to the eighth mode is correct, all couplings would have been zero.

IV. SUMMARY

We have demonstrated that because the orientational disorder breaks the momentum conservation, Raman measurements of the H_g modes in the A_3C_{60} should see a broadening due to the decay in electron-hole pairs. This enables Raman scattering experiments to derive electron-phonon coupling strengths. Furthermore, the explicit calculation shows that the width of this $\mathbf{q}=0$ mode is not very different from the \mathbf{q} -averaged width, where the latter is described by Allen's formula. We further find that the local "anti-ferromagnetic" correlation of the molecular orientation is important for obtaining the non-symmetric line-shape seen experimentally. This provides support for such a local correlation actually taking place in the real system. This leads to a large splitting between a two-fold and a three-fold degenerate component. Experimentally additional structures are seen which are not reproduced by the present calculations. It would therefore be interesting to include corrections to Migdal's theorem beyond the present calculations, and effects of the Coulomb interaction.

This work has been supported by the Max-Planck-Forschungspreis.

w_{ph}	$\Delta\omega_{ph}$	γ_{ph}	$\Delta\omega_{Allen}$	γ_{Allen}
0.03	-0.0076	0.00328	-0.0076	0.00217
0.04	-0.0064	0.00402	-0.0074	0.00290
0.05	-0.0063	0.00460	-0.0073	0.00362
0.06	-0.0062	0.00560	-0.0071	0.00435

TABLE I. Phonon level shifts and broadening from numerical estimates and Allen's formula. The numerical estimates are from fitting of $\mathbf{q}=0$ spectral function (see text) and the estimates from Allen's formula use Eqs. (15-16) with $N(0) = 6.2$ per eV and $g = 0.03$ eV.

V. APPENDIX: COEFFICIENTS $c_{\mu\nu}^{ij}$ FOR RAMAN SCATTERING

In the Raman scattering experiment ($\mathbf{q} = 0$), the incoming light with energy ω_i is scattered by losing the energy of ω_{ph} to the phonon in solid. Following Quang *et al.*²³, we treat the photon classically. The scattering rate $I_p(\omega_i, \omega_{ph})$ with a polarization vector p can then be expressed as

$$I_p(\omega_i, \omega_{ph}) \propto \sum_{\alpha, \alpha'} \text{Im} D_{\alpha, \alpha'}(\omega_{ph}) h_{\alpha}^p(\omega_i, \omega_{ph}) h_{\alpha'}^p(\omega_i, \omega_{ph})^*, \quad (22)$$

where $h_{\alpha}^p(\omega_i, \omega_{ph})$ is given by, as depicted in Fig. 3,

$$h_{\alpha}^p(\omega_i, \omega_{ph}) = \sum_{n, m, l} g_{nm}^{\alpha} P_{nl}^p P_{ml}^p \times \int d\omega G_n^0(\omega) G_m^0(\omega + \omega_{ph}) G_l^0(\omega + \omega_i), \quad (23)$$

with matrix elements P_{nl}^p of the dipole moment operator at the polarization p between non-interacting electronic eigenstates n and m . We consider the transitions $t_{1u} \rightarrow t_{1g}$, since these transitions have large dipole matrix elements. Since a typical frequency of the light source is a few eV, and the $t_{1u} - t_{1g}$ splitting is only about $\Delta_t \sim 1$ eV, transitions to higher states may, however, also play a role.

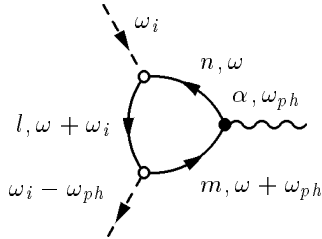


FIG. 3. Effective photon-phonon interaction vertex. The incoming photon (dashed lines) with frequency ω_i scatters to a photon with frequency $\omega_i - \omega_{ph}$ by losing its energy to the α -th phonon mode (wavy line) with energy ω_{ph} . The interaction is mediated by the electrons (thick lines labelled as n, m, l) in the partially filled t_{1u} band and in the empty t_{1g} band in the solid. The filled dot represents the electron-phonon interaction with strength g_{nm}^{α} and the empty dots the electron-photon dipole interaction.

We make an approximation to $h_{\alpha}^p(\omega_i, \omega_{ph})$ where the intermolecular hoppings are ignored due to their relatively small bandwidth. Then, the indices in the integrand in Eq. (23) refer to orbitals on the same site. Since the three orbitals in t_{1u} or t_{1g} -orbitals are all equivalent and the integral depends on the indices only through their energies, the integral is only a function of $\omega_i, \omega_{ph}, \Delta_t$. Furthermore, since $\omega_i \gg W$ and $\omega_{ph} < W$

with the bandwidth $W \sim 0.5$ eV, we ignore the ω_i, ω_{ph} dependency in $h_{\alpha}^p(\omega_i, \omega_{ph})$. Now factoring out the integral, we have

$$h_{\alpha}^p(\omega_i, \omega_{ph}) = \frac{g}{2} \sum_{i, n, m, l} V_{nm}^{(\mu)} P_{i, nl}^p P_{i, ml}^p, \quad (24)$$

where the matrix elements P_{nl}^p in Eq. (23) are reduced to matrix elements between local orbitals n, l at site i , $P_{i, nl}^p$.

We denote the three t_{1u} and t_{1g} -molecular orbitals as x, y, z , as in Ref. 24. For the first type of orientation, we can easily understand from symmetry of C_{60} molecules that

$$P_{i, xy}^p = p_z, \quad P_{i, yz}^p = p_x, \quad P_{i, zx}^p = p_y \quad (\text{orient. 1}) \quad (25)$$

for a polarization direction $\mathbf{p} = (p_x, p_y, p_z)$ with $|\mathbf{p}| = 1$. Similarly for the second type of orientation, we only need to rotate the molecule 90 degree along z -axis, which gives

$$P_{i, xy}^p = p_z, \quad P_{i, yz}^p = -p_y, \quad P_{i, zx}^p = p_x \quad (\text{orient. 2}). \quad (26)$$

Note that $P_{i, nn}^p = 0$. Therefore, leaving out common factors, we can write using Eq. (3),

$$h_{i1}^p(\omega_i, \omega_{ph}) = p_x^2 + p_y^2 - 2p_z^2, \quad p_x^2 + p_y^2 - 2p_z^2 \quad (27)$$

$$h_{i2}^p(\omega_i, \omega_{ph}) = \sqrt{3}(p_y^2 - p_x^2), \quad -\sqrt{3}(p_y^2 - p_x^2) \quad (28)$$

$$h_{i3}^p(\omega_i, \omega_{ph}) = 2\sqrt{3}p_x p_y, \quad -2\sqrt{3}p_x p_y \quad (29)$$

$$h_{i4}^p(\omega_i, \omega_{ph}) = 2\sqrt{3}p_y p_z, \quad 2\sqrt{3}p_z p_x \quad (30)$$

$$h_{i5}^p(\omega_i, \omega_{ph}) = 2\sqrt{3}p_z p_x, \quad -2\sqrt{3}p_y p_z, \quad (31)$$

where the first expressions on the right hand side are for molecules of orientation of type 1 and the second for type 2.

Finally, we take average of $h_{i\mu}^p h_{j\mu'}^p$ over the polarization directions, *i.e.*, $\langle h_{i\mu}^p h_{j\mu'}^p \rangle = \int \frac{d\Omega_p}{4\pi} h_{i\mu}^p h_{j\mu'}^p$. Defining $c_{\mu\mu'}^{ij} = \frac{5}{4} \langle h_{i\mu}^p h_{j\mu'}^p \rangle$, we obtain c as given in Eqs. (10-13). Then

$$\langle I_p(\omega_i, \omega_{ph}) \rangle_p \propto \sum_{\alpha} \text{Im} \tilde{D}_{\alpha, \alpha}(\omega_{ph}), \quad (32)$$

with $\tilde{D}_{\alpha, \alpha}$ defined in Eg. (9).

Now, we look for the Dyson equation corresponding to the reduced Greens function $\tilde{D}_{\nu, \nu}(\mathbf{q}, \omega)$ at $\mathbf{q}=0$. we can rewrite $\tilde{D}_{i\mu, j\nu}$ by splitting the coefficient matrix $c_{\mu\nu}^{ij}$ as

$$\tilde{D}_{i\mu, j\nu} \equiv \sum_{\nu'} c_{\mu\nu'}^{ij} D_{i\nu', j\nu} = \sum_{\nu', \nu''} \bar{\tau}_{\mu\nu'}^i D_{i\nu', j\nu''} \tau_{\nu''\nu}^j, \quad (33)$$

where $\tau_{\mu\nu}^i$ is the 5×5 matrix defined as the unit matrix for $o(i) = 1$ and

$$\begin{pmatrix} 1 & 0 & 0 & 0 & 0 \\ 0 & -1 & 0 & 0 & 0 \\ 0 & 0 & -1 & 0 & 0 \\ 0 & 0 & 0 & 0 & -1 \\ 0 & 0 & 0 & 1 & 0 \end{pmatrix} \quad \text{for } o(i) = -1,$$

and $\bar{\tau}^i = (\tau^i)^{-1}$. Now employing the matrix notation for the orbital indices,

$$\tilde{D}_{ij} = \bar{\tau}^i \left(D^0 \delta_{ij} + D^0 \sum_k \Pi_{ik} D_{kj} \right) \tau^j \quad (34)$$

$$= D^0 \delta_{ij} + D^0 \sum_k \bar{\tau}^i \Pi_{ik} \tau^k \bar{\tau}^k D_{kj} \tau^j \quad (35)$$

$$= D^0 \delta_{ij} + D^0 \sum_k \tilde{\Pi}_{ik} \tilde{D}_{kj}, \quad (36)$$

with the reduced self-energy $\tilde{\Pi}_{i\mu,j\nu}(\omega)$ defined as

$$\tilde{\Pi}_{i\mu,j\nu} = \sum_{\nu'} c_{\mu\nu'}^{ij} \Pi_{i\nu',j\nu}. \quad (37)$$

Finally by taking the summation over site indices i, j , we obtain the reduced phonon self-energy $\tilde{\Pi}_{\mu\nu}(\mathbf{q} = 0, \omega)$ for $\tilde{D}_{\mu\nu}(\mathbf{q} = 0, \omega)$ as Eq. (18).

¹ P.B. Allen, Phys. Rev. B **6**, 2577 (1972); Solid State Commun. **14**, 937 (1974).

² K. Prassides, C. Christides, M.J. Rosseinsky, J. Tomkinson, D.W. Murphy, and R.C. Haddon, Europhys. Lett. **19**, 629 (1992).

³ S. Chakravarty, S. Khlebnikov, and S. Kivelson, Phys. Rev. Lett. **69**, 212 (1992).

⁴ P.W. Stephens, L. Mihaly, P.L. Lee, R.L. Whetten, S.-M. Huang, R. Kaner, F. Diederichs, and K. Holczer, Nature **351**, 632 (1991).

⁵ M.A. Schlüter, M. Lannoo, M.F. Needels, and G.A. Baraff, Phys. Rev. Lett. **69**, 213 (1992).

⁶ M.P. Gelfand, Supercond. Rev. **1**, 103 (1994).

⁷ M.J. Rice and P. Gomes da Costa, in *Electronic Properties of Novel Materials: Progress in Fullerene Research*, Eds. H. Kuzmany, J. Fink, M. Mehring and S. Roth, World Scientific, (Singapore, 1994), p. 501.

⁸ V.L. Aksenov and V.V. Kabanov, Phys. Rev. B **57**, 608 (1998).

⁹ Winter, J. and H. Kuzmany, 1996, Phys. Rev. B **53**, 655.

¹⁰ M.S. Deshpande, E.J. Mele, M.J. Rice, and H.-Y. Choi, Phys. Rev. B **50**, 6993 (1994).

¹¹ O. Gunnarsson, S. Satpathy, O. Jepsen, and O.K. Andersen, Phys. Rev. Lett. **67**, 3002 (1991).

¹² S. Satpathy, V.P. Antropov, O.K. Andersen, O. Jepsen, O. Gunnarsson, and A.I. Liechtenstein, Phys. Rev. B **46**, 1773 (1992).

¹³ I.I. Mazin, A.I. Liechtenstein, O. Gunnarsson, O.K. Andersen, V.P. Antropov, and S.E. Burkov, Phys. Rev. Lett. **26**, 4142 (1993).

¹⁴ Lannoo, M., G.A. Baraff, M. Schluter, and D. Tomanek, 1991, Phys. Rev. B **44**, 12106.

¹⁵ O. Gunnarsson, Phys. Rev. B **51**, 3493 (1995).

¹⁶ V.R. Belosludov, and V.P. Shpakov, Mod. Phys. Lett. B **6**, 1209 (1992).

¹⁷ O. Gunnarsson, Rev. Mod. Phys. **69**, 575 (1997).

¹⁸ S. Teslic, T. Egami, and J.E. Fischer, Phys. Rev. B **51**, 5973 (1995).

¹⁹ A simple Lorentzian fit gives significantly overestimated values for the imaginary part of the self-energy at low frequency peaks.

²⁰ A.S. Alexandrov and V.V. Kabanov, Pis'ma Zh. Eksp. Teor. Fiz. **62**, 920 (1995); Phys. Rev. B **54**, 3655 (1996). In this paper the photoemission spectrum²¹ was described by including the excitation of excitons in addition to the phonons. The exciton energy was estimated for the initial state (C_{60}^-). However, the energy of the exciton in the final state (C_{60}) determines if it is energetically possible to excite an exciton at all in the photoemission process. For the the photon energy studied in Ref. 21 this is not the case, while studies at larger photon energies (W. Eberhardt, priv. commun.) show an exciton at a substantially larger binding energy than assumed by Alexandrov and Kabanov.

²¹ O. Gunnarsson, H. Handschuh, P.S. Bechthold, B. Kessler, G. Ganteför, and W. Eberhardt, Phys. Rev. Lett. **74**, 1875 (1995).

²² The additional structure inside the peak *B* in FIG. 2 appears to be sensitive to the degree of the orientational ordering and merge into one peak as the system size becomes large.

²³ D. N. Quang, B. Esser and R. Keiper, Phys. Stat. Sol. (b) **99**, 103 (1980).

²⁴ N. Laouini, O. K. Andersen, and O. Gunnarsson, Phys. Rev. B **51**, 17446 (1995).